

Streamer and Breakdown Characteristics of Dielectric Liquids Under Impulse Waveforms With Different Tail-Times

Qiang Liu¹, Jing Xiang, Zhongdong Wang², *Fellow, IEEE*, and Olivier Lesaint

Abstract—Impulse waveforms have been widely used in the studies of streamer and breakdown phenomena in dielectric liquids. In this article, both experiments and analyses were carried out to investigate the effects of impulse tail-time on streamer and breakdown characteristics of a mineral oil and a synthetic ester liquid. A range of positive impulse waveforms with the same front-time of 0.8 μs but different tail-times from 8 to 3200 μs were considered. Needle-plane electrodes with a needle tip radius of 10 μm and a gap of 10 mm were used. It was found that reduction of tail-time leads to an increase of 50% impulse breakdown voltage, while the instant breakdown voltage and the time-to-breakdown remain constant. On this basis, an analytical method is developed to estimate the 50% impulse breakdown voltage under waveforms with various tail-times. The method is valid when streamers remain of second mode and in divergent fields. It was also observed that some “self-regulation” by branching explains the constancy of streamer propagation velocity when the applied voltage is increased.

Index Terms—Dielectric liquids, electric breakdown, impulse testing, oil insulation, power transformers, streamer.

I. INTRODUCTION

A VARIETY of transient over-voltages could exist in power networks due to lightning strikes, energization of equipment, and line disconnection. However, for insulation coordination study and factory testing, simplified waveforms, including standard lightning impulse (1.2/50 μs) and standard switching impulse (250/2500 μs), are used. It is debatable on how representative these waveforms are. In contrast, step impulse with fast rise time and long tail-time has been widely

Manuscript received November 12, 2021; accepted March 2, 2022. Date of publication May 17, 2022; date of current version June 27, 2022. (Corresponding author: Qiang Liu.)

Qiang Liu and Jing Xiang are with the Department of Electrical and Electronic Engineering, The University of Manchester, Manchester M13 9PL, U.K. (e-mail: qiang.liu@manchester.ac.uk).

Zhongdong Wang is with the Department of Electrical and Electronic Engineering, The University of Manchester, Manchester M13 9PL, U.K., and also with the College of Engineering, Mathematics and Physical Sciences, University of Exeter, Exeter EX4 4QF, U.K.

Olivier Lesaint is with the Electrical Engineering Laboratory, University Grenoble Alpes, CNRS, Grenoble INP, G2Elab, F-38000 Grenoble, France.

Color versions of one or more figures in this article are available at <https://doi.org/10.1109/TDEI.2022.3173502>.

Digital Object Identifier 10.1109/TDEI.2022.3173502

used in laboratory. It has the advantage to simplify the interpretation of streamer/breakdown results since the applied voltage remains almost constant during the prebreakdown streamer propagation [1]. Breakdown voltage is an important parameter to characterize dielectric liquids. However, due to the complexity of breakdown phenomenon, breakdown voltage is often experimentally determined rather than theoretically estimated.

Previous streamer and breakdown measurements of dielectric liquids were studied under lightning impulse [2]–[7], step impulse [8]–[13], and other impulse waveforms like 2/100 μs [14]. An early study of estimation of impulse breakdown voltage was carried out by considering voltage waveform and streamer propagation [15]. Then, breakdown phenomena observed under lightning impulse and step impulse were compared and discussed in [1] and [16]. Over a large range of gap distances, applied voltage, and liquid nature, the comparison is complex since breakdown occurs from streamers propagating according to different “modes” [17], ranging from second mode (velocity $v \approx 2$ km/s, threshold propagation voltage V_2), third ($v \approx 10$ km/s, V_3), and fourth ($v > 100$ km/s). Parameters such as threshold propagation voltages V_2 , V_3 , vary with distance, and were not yet measured in many liquids [17]. The estimation of breakdown voltage remains a tricky question in the general case.

Below some gap distance (e.g., 12 cm in a mineral oil, 2.5 cm in a natural ester, 5 cm in synthetic ester [1]), breakdown under lightning impulse voltage is due to only second mode streamers, which greatly simplifies analysis. Compared with step impulse voltage, at the same maximum applied voltage under lightning impulse, premature stopping is shown in streamers due to the rapidly decreasing voltage. Hence, a higher maximum applied voltage is required to induce breakdown. In such conditions, it was observed that the voltage V_i at the instant of breakdown approximately equals the breakdown voltage V_b measured under step impulse voltage [1], [16]. This supports the idea of a minimum propagation voltage of second mode streamers.

This article aims to investigate the effects of various impulse tail-times on second mode streamer and breakdown phenomena of dielectric liquids in divergent field (needle-plane) and to develop a method for estimating impulse breakdown voltage in these conditions. Various positive impulse waveforms from the short tail-time of 8 μs to long tail-time of 3200 μs are applied

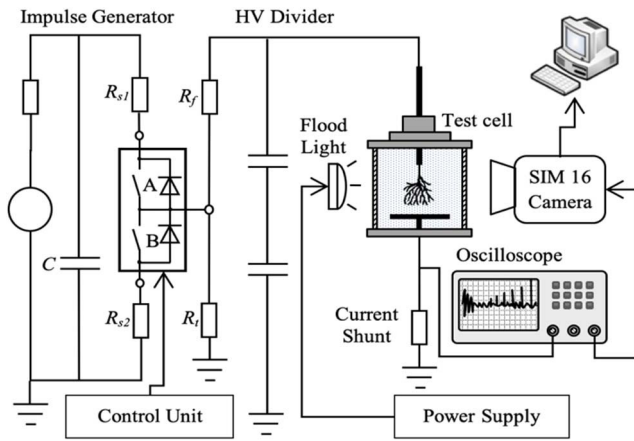


Fig. 1. Schematic of the experimental setup for different impulse waveform tests.

to liquids, using a 10-mm needle-plane gap. At such distance, only second mode streamers are involved in the breakdown process in mineral oil and ester liquid [1]. A 16-channel high-speed camera is used to characterize the streamer stopping length, average propagation velocity, and shape. Comparisons of breakdown voltages (crest value V_c) and instant breakdown voltages V_i between the different impulse waveforms are discussed. An analytical method to estimate the impulse breakdown voltage is developed based on the breakdown results in a mineral oil and then verified by breakdown tests in a synthetic ester liquid.

II. EXPERIMENTAL DESCRIPTIONS

A. Test Setup

The test setup for the present streamer and breakdown investigations under different impulse waveforms is shown in Fig. 1. A high-voltage dc generator was used as dc charging source. A 2-M Ω resistor was installed between the high-voltage dc generator and the solid-state switch to protect the dc source. R_{s1} and R_{s2} are 600- Ω resistors, used to prevent over-current damaging the high-speed switch. A set of replaceable front resistors R_f and tail resistors R_t , allows the generation of various positive impulse waveforms with the same front-time of 0.8 μ s but different tail-times including 8, 14, 30, and 3200 μ s. Once the capacitor is charged, the impulse generator can be triggered by a control unit. A compensated RC voltage divider (North Star VD-100) was used to record impulse voltage waveform. A 10- Ω noninductive current shunt was used to record the current waveform.

A cubic test cell with a total volume of 1 L was used to contain the needle-plane electrodes and liquid sample. The test cell has transparent side walls made of Perspex, which allows observing the streamer and breakdown phenomena by using a high-speed camera. The needle electrode is made of tungsten, etched using an electrochemical technique [18]. Needles with the desired tip radius of 10 μ m were selected by using a microscope. The brass plane electrode has a diameter of 70 mm and an edge radius of 5 mm. The liquid gap between the electrodes is fixed at 10 mm.

A high-speed camera with intensified CCD sensors (Specialized Imaging SIM16) was used to capture the shadowgraph images of streamers. The resolution of the camera setting is 1360 \times 1024 pixels, leading to 0.0215 mm/pixel on streamer images.

B. Liquids Under Investigation

A mineral oil (Gemini X) and a synthetic ester liquid (MIDEL 7131) were studied. Some basic parameters of these liquids can be found in a previous publication [19].

Both dielectric liquids were preprocessed through well-established procedures. A filtering process based on a 0.2- μ m membrane was first used to remove particles. Then, a vacuum process under 500 Pa at 85 $^{\circ}$ C for over 48 h was used to degas and dehydrate the liquid samples. At the end of this procedure, the relative humidity of both liquids is maintained below 10%.

III. PREBREAKDOWN CHARACTERIZATION

Studies of the prebreakdown phenomena, including streamer stopping length and average propagation velocity, were carried out under different positive impulse waveforms. The range of applied voltages covers from near inception to near breakdown levels. The impulse voltage was increased step by step with an increment of 2 kV. At each voltage level, a series of ten prebreakdown streamers were investigated. A 60-s interval was implemented between shots. The liquid sample and the needle electrode were replaced after each set of impulse tests to minimize the potential cumulative effect if there is any.

A. Stopping Length

Stopping length l_s measured in this article is the straight-line distance from the farthest tip point of a streamer to the needle electrode. Fig. 2 shows the comparisons of streamer stopping length in the mineral oil obtained under different waveforms, where 50% breakdown voltages are marked as the reference ($V_{b-8 \mu s}$, $V_{b-14 \mu s}$, $V_{b-30 \mu s}$, and $V_{b-3200 \mu s}$ stand for 50% impulse breakdown voltage with different tail-times, respectively). Quoted voltages refer to the crest value V_c of impulses. The mean and standard deviation are calculated based on ten measurements at each voltage level.

The results indicate that streamer stopping length l_s increases gradually with applied voltage V_c for all impulse waveforms investigated. At the same voltage level, streamers under longer tail impulse propagate much further than under shorter tail-time impulse. Accordingly, breakdown voltages increase with shorter impulses. Fig. 3 shows streamer stopping lengths in the synthetic ester liquid, which follows the similar trends as described in the mineral oil.

B. Average Propagation Velocity

Average propagation velocities v_a of streamers are calculated using two methods. When no breakdown occurs, v_a is calculated by dividing the stopping length by the propagating time, determined from measured current signals; when

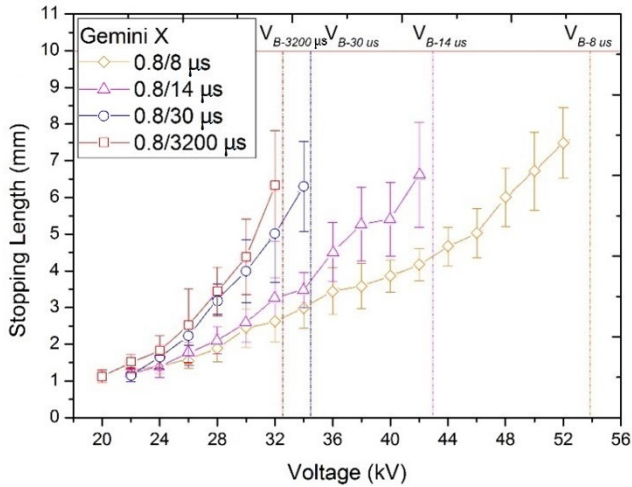


Fig. 2. Stopping length I_s of streamers in mineral oil versus crest applied voltage V_c under different positive impulse waveforms. The error bar represents one standard deviation, the same for other figures.

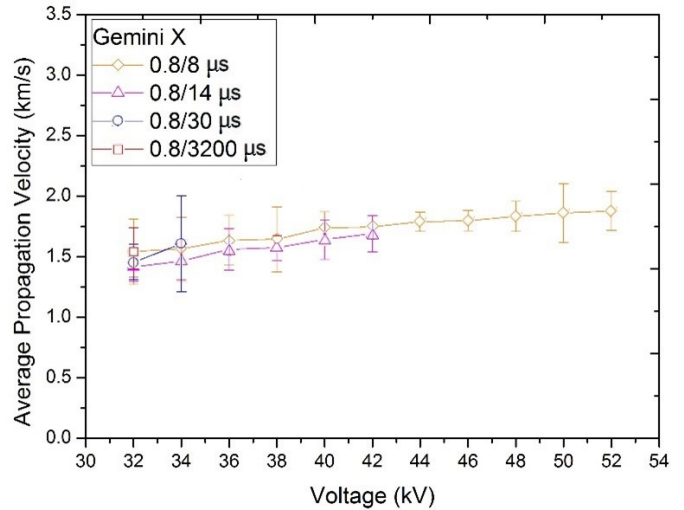


Fig. 4. Average propagation velocity v_a of streamers in mineral oil versus applied voltage V_c under different positive impulse waveforms.

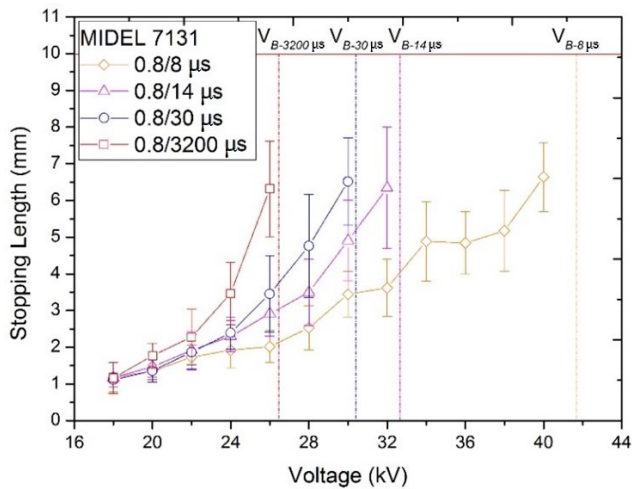


Fig. 3. Stopping length I_s of streamers in synthetic ester versus crest applied voltage V_c under different positive impulse waveforms.

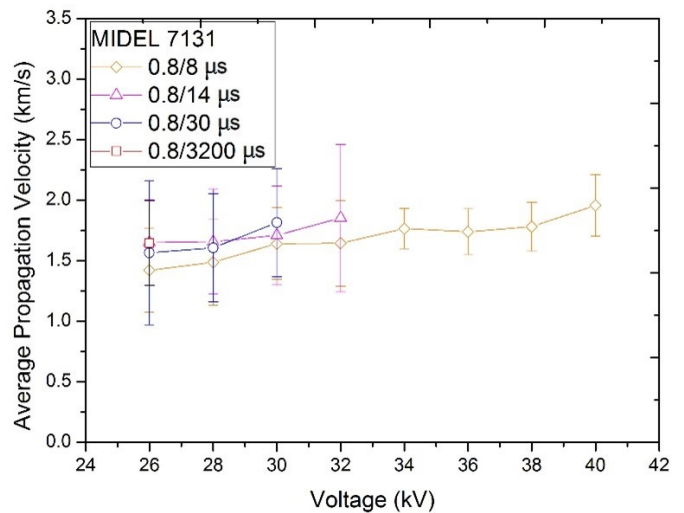


Fig. 5. Average propagation velocity v_a of streamers in synthetic ester versus applied voltage V_c under different positive impulse waveforms.

breakdown occurs, v_a is calculated by dividing the gap distance by the time to breakdown.

Fig. 4 shows the comparison of streamer average propagation velocities in the mineral oil, under different positive impulse waveforms. The average propagation velocities show a small increase (from 1.4 to 1.8 km/s) over the investigated voltage range, and almost no variation when the impulse waveform is changed. Measured velocities confirm that all streamers observed during the tests were of second mode. The similar phenomenon was observed in the synthetic ester liquid, as shown in Fig. 5.

IV. BREAKDOWN TESTS

A. Results of the Mineral Oil

The breakdown voltage was determined based on step increase method, where the applied voltage V_c was increased step by step with an increment of 1 kV per step. Ten breakdowns were carried out for each liquid sample.

A new needle was used for each sample, i.e., each needle experienced maximum ten breakdown events. The breakdown energy was limited by the presence of series resistors R_s and R_f . Some blunting of the needle probably occurred due to repeated breakdown arcs, which may slightly increase its tip radius above the initial 10- μ m value. However, no evolution of measured breakdown voltages (e.g., increase) was noted during the test sequence, as shown in Fig. 6. The fact that the breakdown voltage remained unchanged despite the needle might be modified evidences that breakdown remained of “propagation-controlled” type during the whole sequence: the initiation voltage remained lower than the breakdown voltage. This constitutes an important condition for the validity of the model developed in Sections IV-B and IV-C.

To determine the probability-based breakdown voltage, either Normal or Weibull distribution is employed to fit the breakdown data. In this article, Weibull distribution was chosen as it has been widely used in the field.

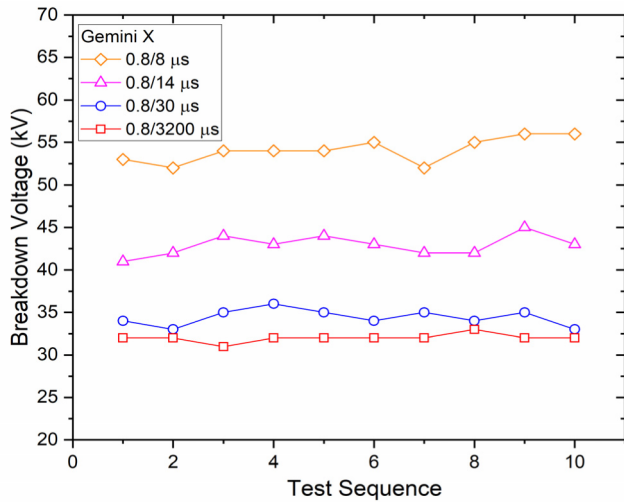


Fig. 6. Chronological order of the breakdown voltages of the mineral oil under different positive impulse waveforms.

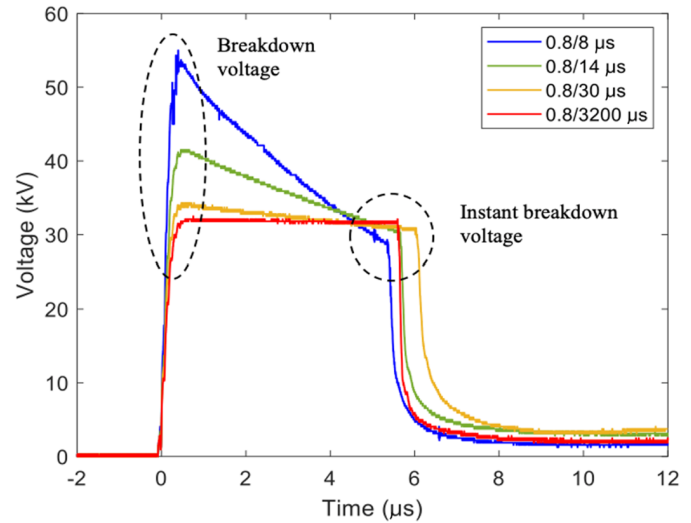


Fig. 8. Typical breakdown waveforms of the mineral oil under different positive impulse waveforms.

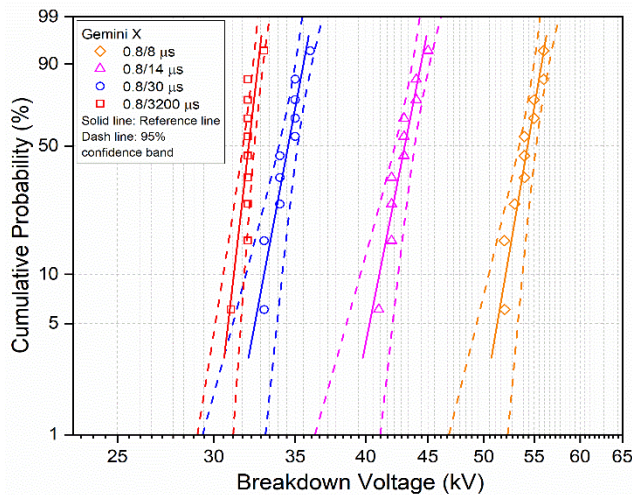


Fig. 7. Weibull plot of breakdown voltages in the mineral oil under different positive impulse waveforms.

TABLE I

WEIBULL PARAMETERS OF BREAKDOWN RESULTS OF THE MINERAL OIL OBTAINED UNDER DIFFERENT POSITIVE IMPULSE WAVEFORMS

Impulse Waveforms	Shape parameter	Scale parameter	50% Breakdown Voltage (kV)
0.8/8 μ s	45.48	54.76	54.1
0.8/14 μ s	39.17	43.46	42.9
0.8/30 μ s	41.40	34.84	34.7
0.8/3200 μ s	56.85	32.22	32.0

Fig. 7 shows Weibull distribution plots of the breakdown data obtained in the mineral oil under different impulse waveforms.

The shape, scale parameters of the Weibull distribution, and the 50% impulse breakdown voltages of the mineral oil obtained under different impulse waveforms are summarized in Table I. It is observed that the 50% impulse breakdown voltage reduces when the impulse tail-time increases.

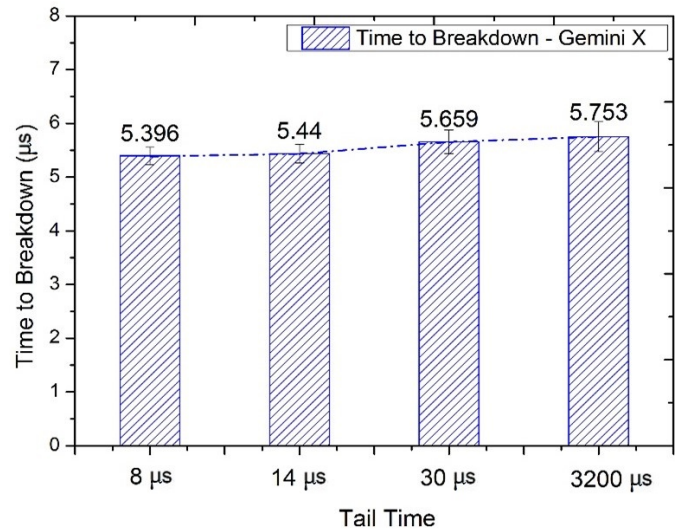


Fig. 9. Time-to-breakdown of the mineral oil under different positive impulse waveforms.

Fig. 8 shows an example of typical breakdown voltage waveforms under each type of impulse waveforms. The time-to-breakdown, t_b , was found to be almost the same for different impulse waveforms. Further detailed results are summarized in Fig. 9. This can be simply explained by the similar streamer average propagation velocity shown in Fig. 4. The crest voltage V_c of the impulse waveform is commonly referred as the breakdown voltage, whereas instant breakdown voltage, V_i , represents the instant voltage when the breakdown occurs. 50% breakdown voltages and instant breakdown voltages obtained under different impulse waveforms are shown in Fig. 10. Although the 50% breakdown voltage reduces with the increase of tail-time, the instant breakdown voltage remains almost unchanged. Logically, the breakdown voltage and instant breakdown voltage under the long tail impulse waveform 0.8/3200 μ s are the same, due to the negligible voltage drop occurring during the streamer propagation.

TABLE II

ESTIMATED BREAKDOWN VOLTAGE AND EXPERIMENTAL BREAKDOWN VOLTAGE OF THE MINERAL OIL OBTAINED UNDER DIFFERENT POSITIVE IMPULSE WAVEFORMS

	Impulse Waveforms	50% Breakdown Voltage (kV)	Estimated Breakdown Voltage (kV)
Input	0.8/8 μ s	54.1	-
	0.8/14 μ s	42.9	38.5
Output	0.8/30 μ s	34.7	33.8
	0.8/3200 μ s	32.0	30.6

B. Estimation of Breakdown Voltage

The behavior in the mineral oil indicates a correlation between breakdown voltage, instant breakdown voltage, time-to-breakdown, and impulse shape. In this case, an analytical method for estimating the breakdown voltage under various impulse waveforms can be established. Equation (1) is widely used to represent impulse voltage waveform [20]

$$v(t) = V(e^{-\alpha t} - e^{-\beta t}) \quad (1)$$

where α and β are used to define impulse voltage waveform.

Based on results shown in Figs. 8–10, it is assumed that V_i and t_b remain the same under impulse waveforms with different tail-times. V_i and t_b can be obtained by conducting breakdown tests under a given impulse waveform and then they can be used to estimate breakdown voltage under another impulse waveform, named as objective impulse waveform.

The proposed analytical method is summarized as follows.

Step 1: Determine parameters V_i and t_b by conducting one set of breakdown tests under a given impulse waveform.

Step 2: Determine parameters α and β of the objective impulse waveform under which breakdown voltage is to be estimated.

Step 3: Find V of the objective impulse waveform when breakdown occurs according to the following equation:

$$V = V_i / (e^{-\alpha t_b} - e^{-\beta t_b}). \quad (2)$$

Step 4: Find breakdown voltage V_c of the objective impulse waveform at $t_{crest} = \ln(\beta/\alpha)/(\beta - \alpha)$ according to the following equation:

$$V_c = V \left(e^{-\alpha \frac{\ln(\beta/\alpha)}{\beta - \alpha}} - e^{-\beta \frac{\ln(\beta/\alpha)}{\beta - \alpha}} \right). \quad (3)$$

In the process of breakdown voltage estimation in the mineral oil, the experimental data of 0.8/8 μ s were selected as the test impulse waveform. The other three impulse waveforms (0.8/14, 0.8/30, and 0.8/3200 μ s) are treated as objective impulse waveforms. Table II summarizes the experimental results of measured 50% breakdown voltages, and estimated breakdown voltages under different impulse waveforms. The results indicate that the estimated breakdown voltages are very close to the experimental results, with a relative difference within 10%. The three objective breakdown voltage waveforms are shown in Fig. 11, where the shapes of the simulated waveforms are identical to the impulse waveforms obtained by experiments shown in Fig. 8.

TABLE III

ESTIMATED BREAKDOWN VOLTAGE AND EXPERIMENTAL BREAKDOWN VOLTAGE OF THE SYNTHETIC ESTER LIQUID OBTAINED UNDER DIFFERENT POSITIVE IMPULSE WAVEFORMS

	Variable Impulse Waveforms	Estimated Breakdown Voltage (kV)	50% Breakdown Voltage (kV)
Input	0.8/3200 μ s	-	26.6
	0.8/8 μ s	42.9	41.7
Output	0.8/14 μ s	32.6	32.9
	0.8/30 μ s	29.4	29.2

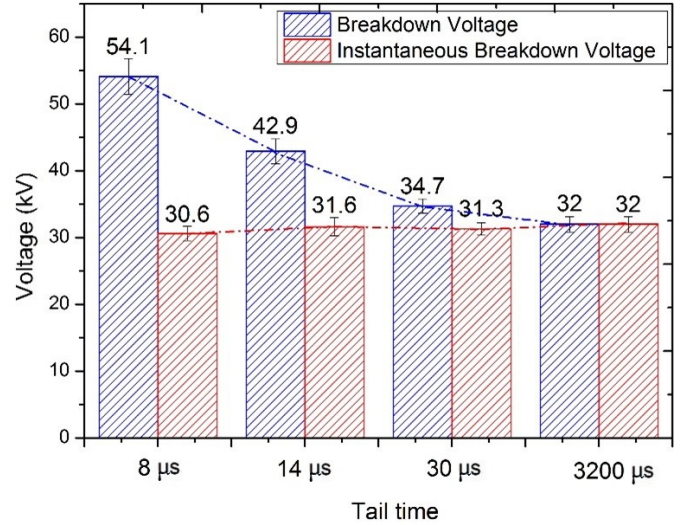


Fig. 10. Breakdown voltage (crest value V_c) and instant breakdown voltages V_i of the mineral oil under different positive impulse waveforms.

C. Verification

To verify the proposed method, another series of breakdown tests was conducted in the synthetic ester liquid. The test conditions, including gap distance, tip radius, electrode configuration, and voltage polarity, are the same. Under impulse waveform 0.8/3200 μ s, the instant breakdown voltage V_i is obtained (26.6 kV), as well as the time-to-breakdown t_b (5.1 μ s). Then, parameters α and β are obtained for the objective impulse waveforms, including 0.8/8, 0.8/14, and 0.8/30 μ s. Finally, with the input values of α , β , V_i , and t_b , the breakdown voltages can be estimated as given in Table III. In addition, the simulated impulse voltage waveforms under breakdown conditions are plotted in Fig. 12.

Breakdown impulse waveforms measured in the same conditions are shown in Fig. 13. Both the waveform shapes and voltage levels are comparable with the simulated ones. The 50% breakdown voltages given in Table III are very close to estimated values, with a relative difference within 3%. Therefore, it is confirmed that the hypotheses used to calculate breakdown voltage (i.e., constant V_i and t_b at fixed gap distance) are also valid for the synthetic ester liquid.

V. DISCUSSION

A series of streamer images were captured with the high-speed camera to analyze streamer propagation and eventual breakdown. With the short tail impulse, higher voltage level

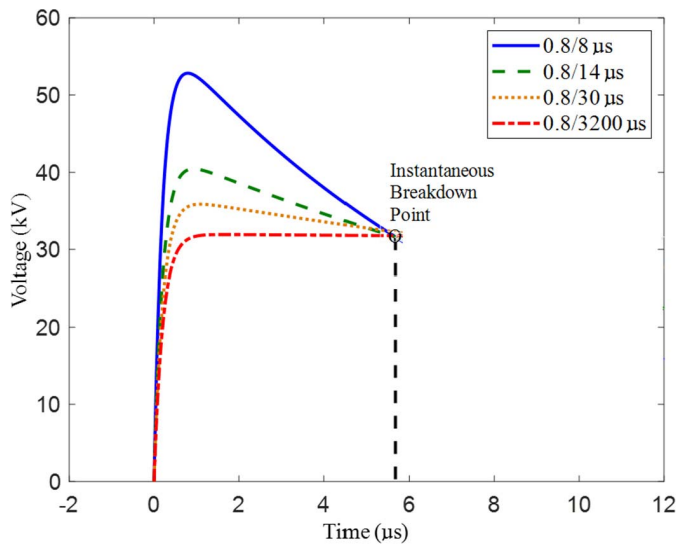


Fig. 11. Simulated different impulse waveforms at breakdowns in the mineral oil, positive polarity.

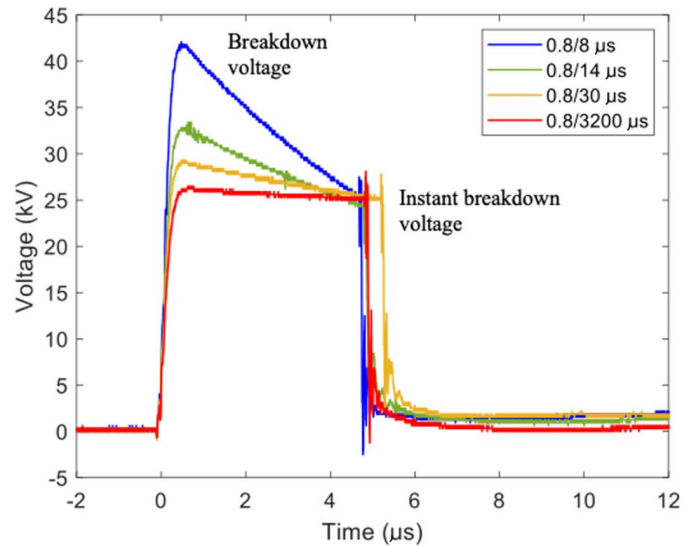


Fig. 13. Typical breakdowns in the synthetic ester liquid under different positive impulse waveforms.

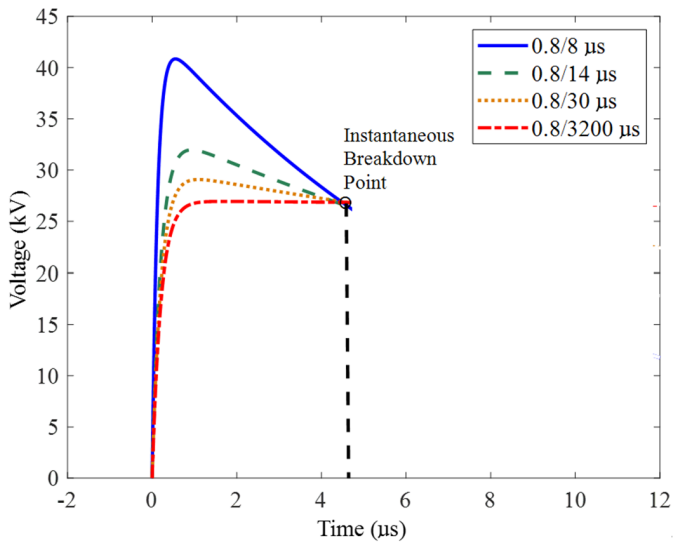


Fig. 12. Simulated different impulse waveforms in the synthetic ester liquid, positive polarity.

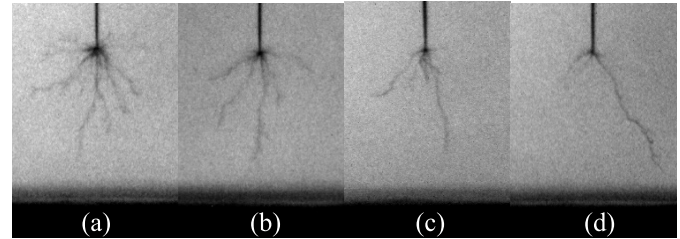


Fig. 14. Streamer in the mineral oil under different positive impulse waveforms (a) 0.8/8 μs , $V = 52$ kV, $I_{\text{stopping}} = 7.62$ mm, (b) 0.8/14 μs , $V = 42$ kV, $I_{\text{stopping}} = 7.71$ mm, (c) 0.8/30 μs , $V = 34$ kV, $I_{\text{stopping}} = 7.44$ mm, and (d) 0.8/3200 μs , $V = 32$ kV, $I_{\text{stopping}} = 7.85$ mm.

is required in order to reach the same streamer stopping length, as compared with longer impulses (see Figs. 2 and 3).

Figs. 14 and 15 show typical images of positive streamers with similar stopping length under different impulse waveforms, in the mineral oil and the synthetic ester, respectively. The stopping lengths of the selected streamers are about 7.44–7.85 mm in the mineral oil, and 6.42–6.59 mm in the synthetic ester. In both liquids, streamers obtained at higher crest voltage V_c under short tail-time impulse show more branches with more small offshoots, as shown in Figs. 14(a) and 15(a). In contrast, only one or two main branches with few small offshoots are observed under long tail-time impulse waveform, as shown in Figs. 14(d) and 15(d).

Figs. 16 and 17 present the streamer areas corresponding to stopped streamers in the mineral oil and the synthetic ester liquid under different positive impulse waveforms.

The streamer area is defined as the apparent area occupied by all streamer branches in the 2-D image, which is estimated using a self-developed program [21]. Accordingly, positive streamers of identical stopping length obtained at higher crest voltage with short tail-time impulse show larger areas when compared with long tail-time impulse. In both liquids, a remarkable constancy of average velocity (evidenced by the constancy of t_b) occurs when V_c is increased.

The influence of ionizable additives (e.g., pyrene) provided a direct evidence about the influence of branching on velocity [22]. Such additives contribute to strongly increasing the degree of branching of second mode streamers. When voltage is raised, the streamer “reacts” by creating more branches, which in turn tends to stabilize the field at filament heads by mutual shielding of branches. Consequently, with additives, the velocity remains remarkably stable over a wide voltage range. In identical conditions without additive, streamers constituted by few branches rapidly accelerate [22]. This “self-regulating” character is especially efficient in mineral oil (that contains ionizable polyaromatics), and much less in other liquids such as esters [1]. The onset of fast streamers is strongly retarded in mineral oils, as compared with ester liquids: the threshold propagation voltage V_3 of third mode streamers is much higher in mineral oil than in ester liquids.

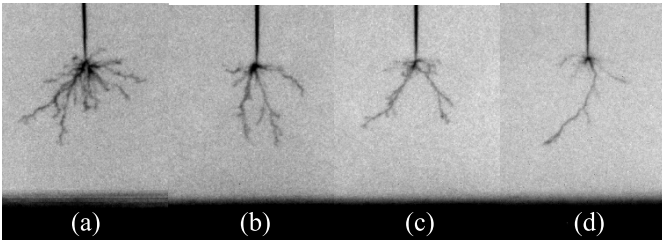


Fig. 15. Streamer in the synthetic ester liquid under different positive impulse waveforms (a) 0.8/8 μs , $V = 40$ kV, $l_{\text{stopping}} = 6.59$ mm, (b) 0.8/14 μs , $V = 32$ kV, $l_{\text{stopping}} = 6.42$ mm, (c) 0.8/30 μs , $V = 30$ kV, $l_{\text{stopping}} = 6.47$ mm, and (d) 0.8/3200 μs , $V = 26$ kV, $l_{\text{stopping}} = 6.57$ mm.

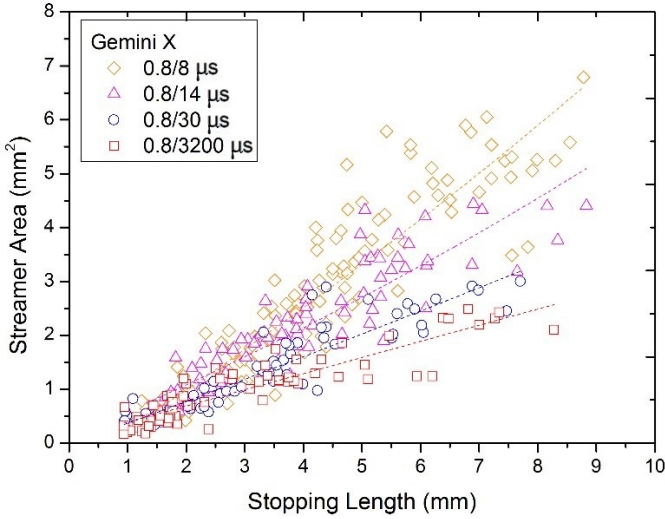


Fig. 16. Positive streamer area as a function of stopping length of the mineral oil under different positive impulse waveforms.

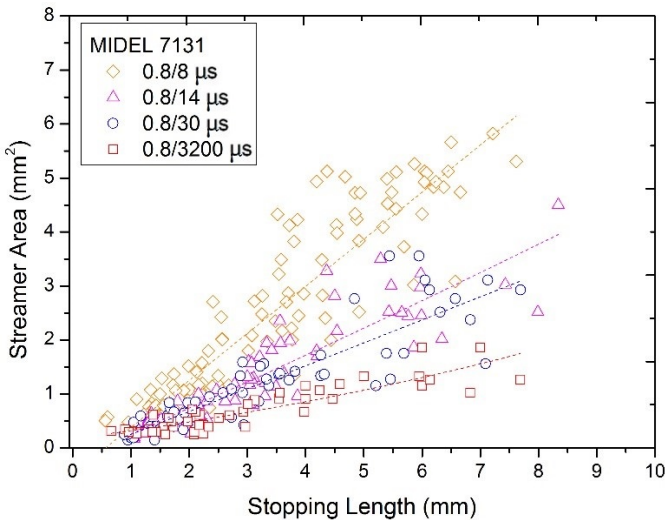


Fig. 17. Positive streamer area as a function of stopping length of the synthetic ester liquid under different positive impulse waveforms.

Photographs in Figs. 14 and 15 suggest that this self-regulation of velocity by branching occurred in our conditions. At the lowest voltage allowing propagation up to the plane (with 3200- μs tail-time impulse), only one branch can propagate. Above this minimum voltage, with short tail-time

impulses, branching occurs and stabilizes velocity. The fact that streamers remained of second mode even in the synthetic ester, although this liquid is less resistant to the fast streamers than the mineral oil, agrees with previous measurements. In [17], values of V_3 in a natural ester extrapolated to the distance of 1 cm indicate that fast streamers should occur above ≈ 50 kV, i.e., a value not reached in our measurements (see Table III). Values of V_3 in the synthetic ester investigated here are not yet known. However, since the synthetic ester is slightly more “stable” than natural esters (streamers remain of second mode at larger distances and higher voltage [22]), the values of V_3 should be larger than in natural ester, and it is logical that no acceleration occurred in the synthetic ester in our conditions.

The fact that minimum propagation voltage in the mineral oil (32 kV) is slightly higher than in the synthetic ester (27 kV) agrees with previous estimations at larger distance [1].

It is clear that the analytical method presented here will not anymore be valid at larger distances and higher applied voltage, when the applied voltage V_c exceeds the threshold propagation voltage of faster streamers V_3 . The validity domain of the model (not yet investigated) should extend to much larger distances in mineral oil, as compared with ester liquids. In [1], breakdown measurements with a long duration 0.4/1400 μs impulse provide values of the minimum propagation voltage of second mode streamers in mineral oil up to 20-cm distance. The basic hypothesis that the instant breakdown voltage V_i under lightning impulse corresponds to this minimum voltage was verified in mineral oil up to 12-cm distance.

Another mandatory condition for the validity of the method is that breakdown must be “propagation controlled.” This means that streamers already occur at voltages below breakdown voltage, typically in divergent fields.

VI. CONCLUSION

Streamer and breakdown characteristics of stopping length, average propagation velocity, streamer shape, and breakdown voltage under positive impulse waveforms with different tail-times of 8, 14, 30, and 3200 μs were investigated in a mineral oil and a synthetic ester liquid.

Compared with the impulses with a long tail-time, reduction of tail-time leads to an increase of 50% impulse breakdown voltage, while the instant breakdown voltage and the time-to-breakdown remain constant. Based on these hypotheses, an analytical method for breakdown voltage estimation under impulse voltage with different tail times has been described in detail, and its validity verified in two liquids. Two conditions must be fulfilled to ensure the validity of such method: prebreakdown streamers must remain of second mode, and the electrode geometry must be divergent enough to ensure a “propagation-controlled” breakdown.

At the prebreakdown stage, time-resolved photographs confirmed that some “self-regulation” of streamer velocity by branching occurred, when the applied voltage exceeded the minimum value allowing the complete propagation of a single streamer branch to breakdown.

REFERENCES

- [1] A. Denat, O. Lesaint, and F. M. Cluskey, "Breakdown of liquids in long gaps: Influence of distance, impulse shape, liquid nature, and interpretation of measurements," *IEEE Trans. Dielectr. Electr. Insul.*, vol. 22, no. 5, pp. 2581–2591, Oct. 2015.
- [2] Y. Kamata and Y. Kako, "Flashover characteristics of extremely long gaps in transformer oil under non-uniform field conditions," *IEEE Trans. Electr. Insul.*, vol. EI-15, no. 1, pp. 18–26, Feb. 1980.
- [3] R. Liu and C. Tornkvist, "Ester fluids as alternative for mineral oil: The difference in streamer velocity and LI breakdown voltage," in *Proc. IEEE Conf. Electr. Insul. Dielectr. Phenomena (CEIDP)*, Aug. 2009, pp. 543–548.
- [4] Q. Liu and Z. Wang, "Streamer characteristic and breakdown in synthetic and natural ester transformer liquids under standard lightning impulse voltage," *IEEE Trans. Dielectr. Electr. Insul.*, vol. 18, no. 1, pp. 285–294, Feb. 2011.
- [5] V.-H. Dang, A. Beroual, and C. Perrier, "Investigations on streamers phenomena in mineral, synthetic and natural ester oils under lightning impulse voltage," *IEEE Trans. Dielectr. Electr. Insul.*, vol. 19, no. 5, pp. 1521–1527, Oct. 2012.
- [6] W. Lu and Q. Liu, "Prebreakdown and breakdown mechanisms of an inhibited gas to liquid hydrocarbon transformer oil under positive lightning impulse voltage," *IEEE Trans. Dielectr. Electr. Insul.*, vol. 23, no. 4, pp. 2450–2461, Aug. 2016.
- [7] W. Lu, Q. Liu, and Z. D. Wang, "Pre-breakdown and breakdown mechanisms of an inhibited gas to liquid hydrocarbon transformer oil under negative lightning impulse voltage," *IEEE Trans. Dielectr. Electr. Insul.*, vol. 24, no. 5, pp. 2809–2818, Oct. 2017.
- [8] P. Rain and O. Lesaint, "Prebreakdown phenomena in mineral oil under step and AC voltage in large-gap divergent fields," *IEEE Trans. Dielectr. Electr. Insul.*, vol. 1, no. 4, pp. 692–701, Aug. 1994.
- [9] O. Lesaint and G. Massala, "Positive streamer propagation in large oil gaps: Experimental characterization of propagation modes," *IEEE Trans. Dielectr. Electr. Insul.*, vol. 5, no. 3, pp. 360–370, Jun. 1998.
- [10] C. T. Duy, O. Lesaint, A. Denat, and N. Bonifaci, "Streamer propagation and breakdown in natural ester at high voltage," *IEEE Trans. Dielectr. Electr. Insul.*, vol. 16, no. 6, pp. 1582–1594, Dec. 2009.
- [11] N. V. Dung, H. K. Hoidalen, D. Linhjell, L. E. Lundgaard, and M. Unge, "Influence of impurities and additives on negative streamers in paraffinic model oil," *IEEE Trans. Dielectr. Electr. Insul.*, vol. 20, no. 3, pp. 876–886, Jun. 2013.
- [12] D. Linhjell, L. E. Lundgaard, M. Unge, and O. Hjortstam, "Pressure-dependent propagation of streamers under step voltage in a long point-plane gap in transformer oil," *IEEE Trans. Dielectr. Electr. Insul.*, vol. 27, no. 5, pp. 1595–1603, Oct. 2020.
- [13] L. E. Lundgaard, D. Linhjell, and G. Berg, "Streamer/leaders from a metallic particle between parallel plane electrodes in transformer oil," *IEEE Trans. Dielectr. Electr. Insul.*, vol. 8, no. 6, pp. 1054–1063, Dec. 2001.
- [14] H. Yamashita, H. Amano, and T. Mori, "Optical observation of pre-breakdown and breakdown phenomena in transformer oil," *J. Phys. D, Appl. Phys.*, vol. 10, no. 13, p. 1753, 1977.
- [15] S. Rząd, J. Devins, and R. Schwabe, "Transient behavior in transformer oils: Prebreakdown and breakdown phenomena," *IEEE Trans. Electr. Insul.*, vol. EI-14, no. 6, pp. 289–296, Dec. 1979.
- [16] Q. Liu, Z. D. Wang, and O. Lesaint, "Comparison of streamer propagation in mineral oils under lightning and step impulse voltages," in *Proc. IEEE 18th Int. Conf. Dielectr. Liquids (ICDL)*, Jun. 2014, pp. 1–4.
- [17] O. Lesaint, "Prebreakdown phenomena in liquids: Propagation 'modes' and basic physical properties," *J. Phys. D, Appl. Phys.*, vol. 49, no. 14, Apr. 2016, Art. no. 144001.
- [18] W.-T. Chang, I.-S. Hwang, M.-T. Chang, C.-Y. Lin, W.-H. Hsu, and J.-L. Hou, "Method of electrochemical etching of tungsten tips with controllable profiles," *Rev. Sci. Instrum.*, vol. 83, no. 8, Aug. 2012, Art. no. 083704.
- [19] Q. Liu and Z. Wang, "Streamer characteristic and breakdown in synthetic and natural ester transformer liquids with pressboard interface under lightning impulse voltage," *IEEE Trans. Dielectr. Electr. Insul.*, vol. 18, no. 6, pp. 1908–1917, Dec. 2011.
- [20] E. Kuffel, W. S. Zaengl, and J. Kuffel, *High Voltage Engineering Fundamentals*. Oxford, U.K.: Butterworth-Heinemann, 2000.
- [21] Z. Liu, Q. Liu, and Z. D. Wang, "Effect of electric field configuration on streamer and partial discharge phenomena in a hydrocarbon insulating liquid under AC stress," *J. Phys. D, Appl. Phys.*, vol. 49, no. 18, May 2016, Art. no. 185501.
- [22] O. Lesaint and M. Jung, "On the relationship between streamer branching and propagation in liquids: Influence of pyrene in cyclohexane," *J. Phys. D, Appl. Phys.*, vol. 33, no. 11, p. 1360, 2000.